Appl. Phys. B 27, 129–135 (1982)

Applied Physics B Photophysics and Laser Chemistry

Mass-Selective Trapping of Pulsed Charged Particle Beams

Chun-Sing O and H. A. Schuessler

Department of Physics, Texas A & M University, College Station, TX 77843, USA

Received 7 September 1981/Accepted 1 December 1981

Abstract. The phase-space method is used to evaluate the mass-selective ion confinement properties of the radio-frequency (rf) quadrupole ion trap with phase-synchronized switching-on of the driving rf field for pulsed ion injection from an external source. The results are of interest for on-line investigations of both short-lived isotopes and stable highly charged ions. In particular, singly charged ions with an energy of 10 eV and a mass in the neighborhood of 100 amu, injected along the gap or through an aperture on one of the electrodes, are considered. Mass-selective storage of the injected ions is possible for any trap operation point within the stability region by allowing a field-free drift distance before ion injection. It is shown that after appropriate scaling the results apply to the trapping of any pulsed beam of charged particles.

PACS: 07.75

Presently considerable effort is directed at nuclear studies of highly unstable nuclei far off the region of β-stability [1]. A number of investigations have already been carried out on-line with nuclear accelerators [2] and were made possible by recent developments in producing a wide range of intense ion beams of short-lived nuclei [3] and by the introduction of novel nuclear [4] and atomic [5] physics techniques. In addition, highly charged stable ions have been produced in high-energy heavy ion reactions [6] and make investigations of, for instance, fundamental QED contributions to the hyperfine structure of hydrogen-like highly charged ions possible. For the study of both short-lived isotopes and high charge state ions it is convenient and often even necessary to study only one nuclear species at a time. However, since nuclear reactions produce several elements, isotopes, and charge states at once, the newly produced nuclides and highly charged ions must be mass and charge separated on-line to the production facility.

It is expected that the present sensitivity of experiments of about 10^5 ions/s [7] can be increased by orders of magnitude if the ions can be caught in flight as they emerge from a nuclear reaction. Experimental work to demonstrate the techniques is now in progress in our laboratory. The usefulness of ion-storage techniques would be increased if, in addition, mass selective storage could be effected. In such a case the usual on-line mass separator would not be required. The present work presents a model calculation of mass-selective ion storage using a radio-frequency quadrupole ion trap and a pulsed low energy ion beam. The ion beam is available after suitable collection and deceleration [8] of ions produced in a variety of nuclear reactions. The relevant properties of an on-line ion trap are then collection efficiency, since there is a minimum abundance requirement for the study of an unstable isotope or highly charged ion under investigation, and the resolving power, which is related to the isotopic or charge state purity.

Section 1 briefly summarizes the theory of the rf quadrupole trap. In Sect. 2 the mass selectivity of ions already confined in the rf quadrupole ion trap is discussed. The numerical results of mass selective storage of injected ions are presented in Sect. 3.

1. Theory of the rf Quadrupole Ion Trap

The theory and the construction of the three-dimensional rf quadrupole trap have been reviewed extensively [9, 10], so that only a short summary of the principle of operation is given here. Basically a three-

0721-7269/82/0027/0129/$01.40

dimensional potential well is generated to confine the ions by applying a suitable combination of ac and dc driving voltages to the ion trap electrodes. The quadrupole electrode arrangement consists of a central doughnut-shaped ring electrode and two end cap electrodes with complementary hyperbolic cross sections. The electrodes are positioned in such a way that the dimension from the center of the trap to the midpoint of the ring electrode r_0 and half of the separation between the apexes of the two end cap electrodes z_0 satisfy the relation $r_0^2=2z_0^2$. A potential difference being the superposition of a constant dc bias U_0 and an ac voltage with amplitude V_0 and oscillation angular frequency Ω, namely,

$$U(t)=U_0-V_0\cos\Omega t \tag{1}$$

is maintained between the ring and the end cap electrodes. When the driving voltage $U(t)$ is applied to the end cap electrodes with the ring electrode grounded, the three-dimensional quadrupole field inside the ion trap is given by

$$V(x,y,z)=\frac{U_0-V_0\cos\Omega t}{r_0^2}\left(z^2-\frac{x^2+y^2}{2}\right). \tag{2}$$

The equation of motion in each direction for an ion of charge-to-mass ratio e/m inside the ion trap can be written in the form of the Mathieu equation

$$\frac{d^2u}{d\xi^2}+[a_u-2q_u\cos 2(\xi-\xi_0)]u=0. \tag{3}$$

Here u is any one of the three coordinates x, y, and z; ξ_0 is the initial phase of the driving rf field, and $\xi=(1/2)\Omega t$ is the transformed time. The quantities a_u and q_u determine the stability property of the solutions of the Mathieu equation and are called the stability parameters. These parameters are defined as

$$a_z=-2a_x=-2a_y=8eU_0/mr_0^2\Omega^2 \tag{4a}$$

and

$$q_z=-2q_x=-2q_y=4eV_0/mr_0^2\Omega^2. \tag{4b}$$

For the ion motion to be stable in a given direction the ion trap operational conditions must be chosen so that the two stability parameters are in the region of stable solutions of the Mathieu equation. To determine the stability conditions in all three directions of motion the appropriate regions of stability are scaled and then superimposed on one another. The resultant stability diagram, given in terms of a_z and q_z, is depicted in Fig. 1a. The four curve boundary lines define the region of values of a_z and q_z for stable ion motion inside the rf quadrupole trap. Not all ions with a stable trajectory can be confined. For an ion to be trapped indefinitely the maximum amplitude of the stable ion trajectory must also be smaller than the corresponding characteristic dimension of the trap. Otherwise the ion hits one of the electrodes and is lost. Matrix techniques based on phase-space dynamics [11, 12], similar to those used for a high energy accelerator design, have been employed successfully to determine the maximum motional amplitudes of an ion in the rf quadrupole trap. The matrix in question is written, for each set of a_u, q_u, and ξ_0, as

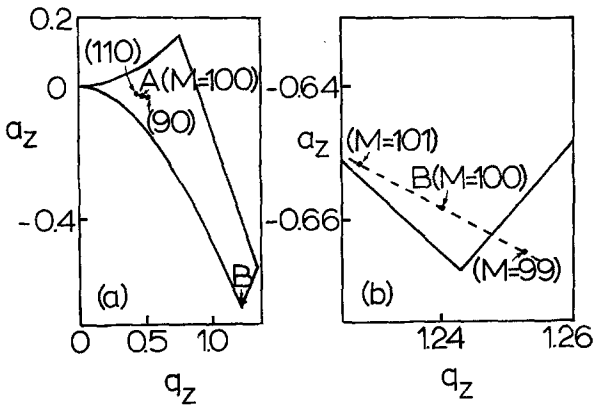

Fig. 1. (a) Stability diagram for a radio-frequency quadrupole trap showing the positions of the operation point for ions of different masses. (b) Magnified stability diagram near the mass-selective tip

$$M=\begin{bmatrix}\cos\left(\frac{2\pi\omega_u}{\Omega}\right)+\alpha_u\sin\left(\frac{2\pi\omega_u}{\Omega}\right) & \beta_u\sin\left(\frac{2\pi\omega_u}{\Omega}\right)\\ -\gamma_u\sin\left(\frac{2\pi\omega_u}{\Omega}\right) & \cos\left(\frac{2\pi\omega_u}{\Omega}\right)-\alpha_u\sin\left(\frac{2\pi\omega_u}{\Omega}\right)\end{bmatrix}, \tag{5}$$

where $\beta_u\gamma_u-\alpha_u^2=1$. The quantity ω_u in M is the secular frequency of the ion oscillation motion in the u direction and is independent of the initial rf phase ξ_0. On the other hand, the remaining parameters α_u, β_u, and γ_u depend on a_u, q_u, and ξ_0. The matrix M represents the effect of one complete rf cycle of the driving field on the ion so that after n complete rf field cycles the ion position u_n and velocity $\dot{u}_n=(du/d\xi)_n$ are related to their initial values $(u_0, \dot{u}_0)$ by

$$\begin{bmatrix}u_n\\ \dot{u}_n\end{bmatrix}=M^n\begin{bmatrix}u_0\\ \dot{u}_0\end{bmatrix}. \tag{6}$$

The dynamical specifications of the ion motion are represented by a point in phase space. Such representation points, when evaluated after each complete rf

cycle, lie on an ellipse which is described by the equation

$$\gamma_u u^2 + 2\alpha_u u\dot{u} + \beta_u \dot{u}^2 = \varepsilon_u = S_u/\pi . \tag{7}$$

Here S_u is the area of the ellipse and, for the same operation point (a_u, q_u), depends on the initial condition u_0, $\dot{u}_0$, and ξ_0 of the ion. The extreme values of this ellipse in either direction of the phase space are then the maximum displacement $\sqrt{\beta_u \varepsilon_u}$ and the maximum velocity $\sqrt{\gamma_u \varepsilon_u}$. It should be noted that before the completion of a rf cycle the representation points in the phase space can wander out of the boundaries set by these extreme values of the corresponding acceptance ellipse but that they are always within the limits

$$u_{\max} = \sqrt{\beta_{u,\max} \varepsilon_u} \tag{8a}$$

and

$$\dot{u}_{\max} = \sqrt{\gamma_{u,\max} \varepsilon_u} . \tag{8b}$$

Here $\beta_{u,\max}$ and $\gamma_{u,\max}$ are the maximum values of the respective parameters for each chosen set of values (a_u, q_u). The allowed initial conditions for an ion to be indefinitely trapped in the u direction are those for which $u_{\max}$ is less than the corresponding trap dimension u_d, i.e.

$$u_{\max} \leqq u_d . \tag{9}$$

This requires on the one hand that for a given initial position u_0 the initial velocity must be within the region with the limits

$$\dot{u}_{1,2} = -\frac{\alpha_u}{\beta_u} u_0 \pm \frac{1}{\beta_u} \sqrt{\frac{\beta_u}{\beta_{u,\max}} u_d^2 - u_0^2} . \tag{10}$$

On the other hand, for a given initial velocity $\dot{u}_0$ the initial position of the ion must be within a certain zone bounded by

$$u_{1,2} = -\frac{\alpha_u}{\gamma_u} \dot{u}_0 \pm \frac{1}{\gamma_u} \sqrt{\frac{\gamma_u}{\beta_{u,\max}} u_d^2 - \dot{u}_0^2} . \tag{11}$$

These limits depend on the initial phase ξ_0 and the operation point (a_u, q_u) through the parameters α_u, β_u, and γ_u. For an ion to be confined in the rf quadrupole trap the coordinates of the initial ion position must be within the stable zones, as determined by the respective velocity components, in all three directions for the particular initial phase. Operation of the rf quadrupole trap at a different operation point (a_u, q_u) leads to a very different ξ_0 dependence of the phase-space acceptance ellipse parameters, α_u, β_u, and γ_u, as depicted by the solid lines in Fig. 2, and thus to very different boundaries of the stability zones.

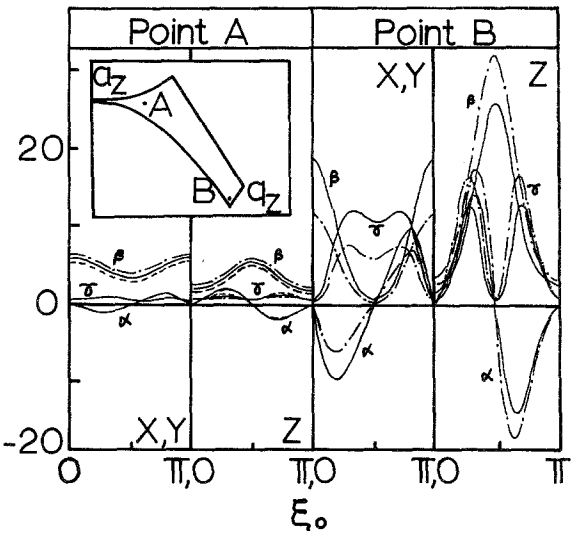

Fig. 2. The phase-space ellipse parameters as functions of the initial rf voltage phase for ions of different masses. The stability parameters for mass 100 ions are $(a_z, q_z) = (-0.0313, 0.5)$ at point A and $(a_z, q_z) = (-0.658, 1.24)$ at point B. The solid lines depict the corresponding curves for mass 100 ions. The dashed and dashed-dotted lines are for ions of masses 90 and 110, respectively, for operation point A. The dashed-dotted lines are for ions of mass 101 at operation point B where ions of mass 99 are out of the stability region

2. Mass Selectivity of Stored Ions

The stability parameters a_z and q_z of the ion motion depend on the mass of the ion in question. Figure 1 shows the different position of the trap operation point for singly charged ions of masses in the neighborhood of 100 amu. If the operation points are within the stability region for the same driving field, ions of neighboring masses can be confined simultaneously. This is the case for the operation point A in Fig. 1a. The values of the stability parameters are $a_z = -0.0313$ and $q_z = 0.5$ for ions of mass 100. Other operation parameters of the rf quadrupole trap are tabulated in Table 1. Because of the slightly different positions of the operation point, the various motional frequencies

Table 1. Operation parameters of the rf quadrupole trap for singly charged ion of mass 100

Radial dimension	$r_0 = 0.54$ cm
Axial dimension	$z_0 = 0.38$ cm
dc bias	$U_0 = -4.7$ V
ac trapping amplitude	$V_0 = 150$ V
Driving frequency	$\Omega = 2\pi \times 1$ MHz
Stability parameters	$q_z = 0.5$
	$a_z = -0.0313$
	$q_x = q_y = -0.25$
	$a_x = a_y = 0.0156$
Axial oscillation frequency	$\omega_z = 2\pi \times 153$ kHz
Radial oscillation frequencies	$\omega_x = \omega_y = 2\pi \times 108$ kHz
Potential well depth	$e\bar{D}_z = e\bar{D}_x = e\bar{D}_y = 16.8$ eV

of inos of the same charge but various masses are different. In this case mass-selective ion detection is still possible by using either the emission or excitation method [13, 14]. In the emission method the energy absorption in a resonantly excited tank circuit leads to a damping, when one of the motional frequencies of a particular ion is tuned through resonance. In the excitation method the coherently excited ion motion is detected by the voltage induced into a broadband passive detection circuit allowing in this way the observation of selectively excited ions over a wide mass range.

Mass-selective ion storage of the rf quadrupole trap, for internally created ions and of a continuous ion beam injected from an external source, is similar to the operation of the two-dimensional quadrupole mass filter. For high mass selectivity an operation point near the lower acute tip of the stability region is usually used, so that ions of neighboring masses are not within the stability region simultaneously [15]. This is the case for the operation point B ($a_z = -0.658$ and $q_z = 1.24$ for mass 100 ions) in Fig. 1b where only singly charged ions of masses 100 and 101 can be trapped. The motion of ions of a higher mass is unstable along the trap axial direction, while that for ions of a lower mass is unstable in the xy plane. However the present study shows that for injection of a pulsed ion beam from an external source into the rf quadrupole ion trap mass-selective ion storage is possible for any operation point within the stability region. This novel feature is possible because the ion trap can be operated similar to a time of flight (TOF) mass spectrometer.

3. Mass Selective Storage of Injected Ions

Ions created externally can be injected into the rf quadrupole trap in two ways: in the continuous mode and in the pulse mode. In the former mode a continuous ion beam is injected into an active quadrupole trap. This possibility has been considered elsewhere [16]. In the pulse mode a pulsed ion beam is injected into the trap when the driving voltage $U(t)$ is off. The quadrupole field is switched on, with the rf driving voltage at a particular initial phase angle ξ_0, after a suitably chosen time delay T_D from the instant of the ion pulse injection. This latter injection mode has been studied using the phase-space method [17, 18].

The present study was carried out to obtain the optimum values of mass resolution and collection efficiency. The numerical calculation was performed at mass 100 for ions confined indefinitely from a pulsed beam of singly charged ions of energy 10 eV and with a circular beam cross section of 1 mm diameter. The pulse duration of the ion beam was assumed to be 1 μs. Hereby the pulse duration includes the combined time spread of the finite time interval of ion creation as well as the arrival time spread due to different positions of ion creation and the energy spread of the ion beam. Three different injection apertures are considered. For gap injection the ion beam travels along the asymptotic lines to the hyperbolic cross sections of the trap electrode surfaces. For radial injection the injection aperture is at the midpoint of the ring electrode and the injection direction is along a radial ray on the equatorial plane. Similarly for axial injection the injection aperture is at the apex of one of the end cap electrodes and the injection direction is along the symmetry axis of the quadrupole structure. Two different trap operation points, A and B for ions of mass 100 indicated in Fig. 1, are used. The former is chosen for favorable ion confinement and represents the symmetric potential well depth mode of operation. The latter is the regular operation point for mass-selective storage of internally created ions. The quadrupole driving voltage $U(t)$ is assumed to be applied to the end cap electrodes. All initial phase angles referrred to here should be replaced by their complementary angles $\xi_0' = \pi - \xi_0$ when $U(t)$ is applied to the ring electrode.

As mentioned in Sect. 1, for an ion with given velocity components to be confined for an indefinite time period in the rf quadrupole trap, the ion position must be on or within a certain critical volume inside the ion trap. Ions located outside of this critical volume when the quadrupole field is turned on will not be trapped. Ions of various masses but the same energy have different travel velocities. In addition, the critical volume depends on the phase space ellipse parameters which, in turn, depend on the operation point and the initial rf voltage phase ξ_0. Ions of neighboring masses correspond to slightly shifted operation point positions within the stability region. This relative shift of the operation point does not introduce significant variations of the phase space ellipse parameters when the trap is operated around point A. However, the effect is prominent around operation point B, as shown in Figs. 2 and 3 where the phase-space ellipse parameters are depicted as functions of the initial rf voltage phase for a couple of ion masses and functions of the ion mass at a given initial rf voltage phase. The critical volume has in general the shape of a rectangular box. A typical example is depicted in Fig. 4 for gap injection of a pulsed beam of ions of different masses and with an energy of 10 eV. The cross-sectional areas of the critical volumes in the xz plane are shown for an initial rf voltage of $\xi_0 = \pi/4$. The two values of the time delay at which the unperturbed straight line ion trajectory intersects the surface of the critical volume for a given ξ_0 determine the time delay interval within which the quadrupole field should be turned on to trap the

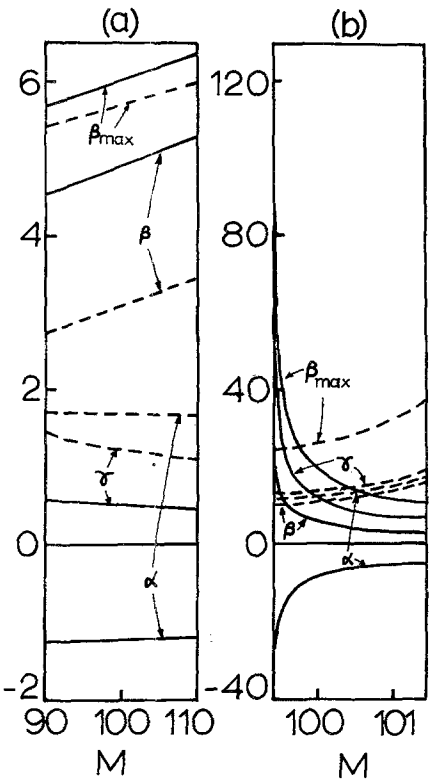

Fig. 3a and b. The phase ellipse parameters as functions of the ion mass. The solid and the dashed lines correspond to the axial and the radial directions, respectively. (a) The operation point is $(a_z, q_z)=(-0.0313, 0.5)$ for ions of mass 100 and an initial phase angle $\xi_0=0.22\pi$, (b) the operation point is $(a_z, q_z)=(-0.658, 1.24)$ for ions of mass 100 and $\xi_0=0.28\pi$

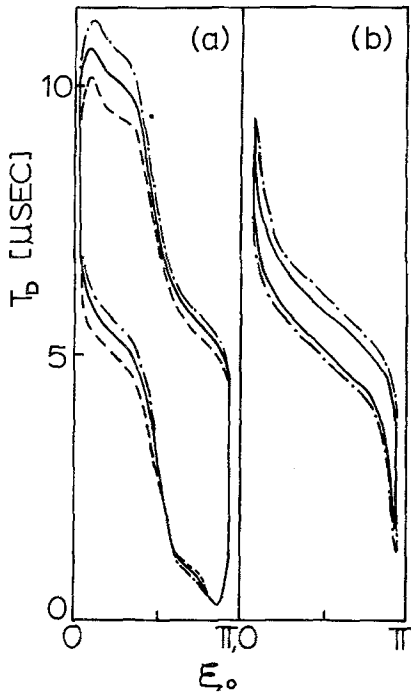

Fig. 5a and b. Time delay interval for ion confinement versus initial rf voltage phase for radial injection. The quadrupole trap is operated at point A in (a) and B in (b). The solid lines are for ions of mass 100 in both figures. The dashed and dashed-dotted lines are for ions of masses 90 and 110, respectively, in a. The dashed-dotted line is for ions of mass 101 in b

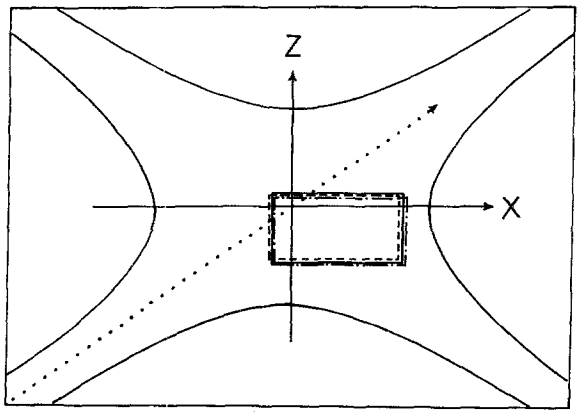

Fig. 4. Cross-sectional areas in the xz plane of the critical volumes for ion confinement in the case of gap injection of ions of 10 eV energy at an initial rf phase $\xi_0=\pi/4$. The trap operation point is $(a_z, q_z)=(-0.0313, 0.5)$. The dashed, solid, and dashed-dotted lines are for ions of masses 90, 100, and 110, respectively. The dotted line represents the unperturbed straight line ion trajectory

injected ions. The results of the calculation for radial injection are presented as T_D versus ξ_0 diagrams for each ion mass in Fig. 5. Corresponding diagrams were also obtained for the axial injection case. However for the gap injection case the calculation showed that while confinement is possible at operation point A, indefinite ion confinement is not possible at point B. For all cases the time delay intervals, during which ion confinement occurs for ions of neighboring masses, overlap one another. The mass resolution of the stored ions alone is therefore not sufficient to trap ions of one isotope only. However, isotope selective ion storage is still possible by taking advantage of the different times of flight ions of the same energy but different masses need to travel a given distance. The quadrupole trap is positioned such that a field-free drift distance exists between the region of ion creation and the injection aperture. Because of the variation in T_d, the time for the same kinetic energy but different masses to travel the distance d, the ions in the same pulse are separated into bunches, when they arrive at the injection aperture. The ions of the lowest mass arrive first and are followed by others with successively higher masses. From the injection aperture it will take each ion an additional time interval T_D to reach the corresponding critical volume in order to be trapped. Since the positions and sizes of the critical volumes for ions of

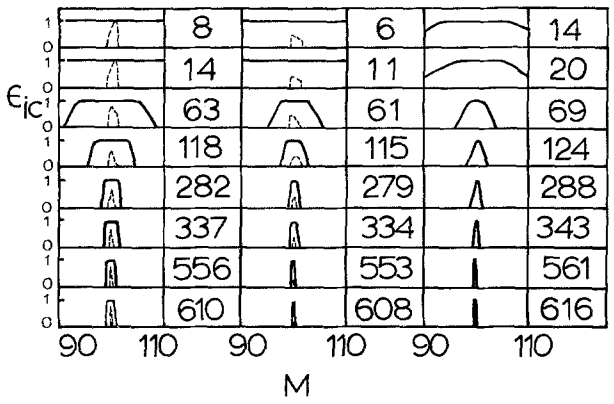

Fig. 6. Ion confinement efficiency versus ion mass curves. The number to the right of each curve is the value of the total time delay to turn on the quadrupole field measured in μs. The drift distance between the ion creation region and the injection aperture, measured in units of r_0, is 0, 1, 10, 20, 50, 60, 100, and 110 from the top to the bottom row. The first column is for radial injection while the second and the third columns are for axial and gap injections, respectively. The solid and the dashed lines are for trap operation points A and B. The initial rf voltage phases are 0.22π, 0.75π, and 0.22π for the solid lines of the three columns from left to right. For the dashed lines $\xi_0 = 0.28\pi$ in both cases

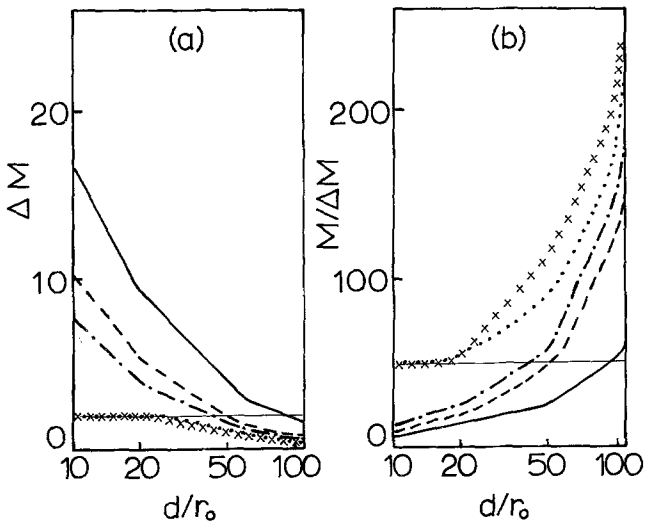

Fig. 7. (a) The mass width, and (b) the mass resolution at an ion mass of 100 are plotted against the drift distance between the ion creation region and the trap injection aperture. The solid, dashed, and dashed-dotted lines are for radial, axial, and gap injection at the trap operation point A. The dotted and the crossed lines are for radial and axial injection at operation point B. The thin horizontal lines represent the values of M and $M/\Delta M$ required to separate ions with masses which differ by 1

the same energy but different masses are different, this is equivalent to the situation of a TOF mass spectrometer with several collectors. Each collector measures a particular ion mass and is set at a different location and has a different gate time. The total time-of-flight, or the total time delay to turn on the quadrupole field measured from ion creation, is now $T_{Dd} = T_D + T_d$. Variation in the values of T_{Dd}, due to changes in either T_D or T_d, leads to mass selectivity of the stored ions. A longer drift distance gives rise to a more extensive spread of the pulsed ion packet, i.e. higher mass selectivity. This behavior is related to the case of energy-selective ion storage from a pulsed ion beam with a large energy spread. The effective time spread which determines the resolution is increased over the ion pulse duration due to the finite duration of the time delay interval for ion confinement.

Typical ion confinement efficiency versus mass curves are depicted in Fig. 6 for different ion injection cases. In the three columns of curves the solid lines are, from left to right, for radial injection at $\xi_0 = 0.22\pi$. Axial injection at $\xi_0 = 0.75\pi$, and gap injection at $\xi_0 = 0.22\pi$, respectively. The trap operation point is around point A of Fig. 1. The corresponding ion confinement curves for the operation point B are shown as dashed lines in the appropriate columns. The value of the initial phase is $\xi_0 = 0.28\pi$. These initial rf phase values are chosen to give a small value of T_D and as the result a higher mass selectivity. The rows in Fig. 6 are for different drift distances between the region of ion creation and the quadrupole trap. The values of d, measured in units of r_0, are 0, 1, 10, 20, 50, 60, 100, and 110 from the top to the bottom row. The results of the corresponding mass width Δm and mass resolution $m/\Delta m$ are summarized in Fig. 7. Here the mass width Δm is defined as the total width of the ion confinement efficiency curve at 10% of the peak efficiency. The thin horizontal lines in Fig. 7 represent the required values of the mass width and the mass resolution at an ion mass 100 to separate ions of masses 99 and 101. The mass resolution improves as the drift distance is increased. When the trap is operated around point A of Fig. 1, gap injection with the minimum T_D values is the most favorable case. However, a drift distance $d = 50\, r_0$, i.e. about 28 cm, is needed to separate neighboring isotope ions. On the other hand, when the trap is operated around point B of Fig. 1 the mass resolution is much higher. Here axial injection (crossed line) leads to better mass resolution at larger drift distances, but slightly lower mass resolution at small drift distances when compared to the corresponding radial injection case (dotted line). In both cases, a drift distance $d = 10\, r_0$, i.e. less than 6 cm, will be sufficient to separate the ions of neighboring isotopes. It must be noted that this improved mass resolution is achieved at the expense of the lower ion confinement efficiency. The peak ion confinement efficiency is about 70% and 40% for the radial and axial injections, respectively, when the operation point B is used compared with the value of 100% at operation point A.

4. Conclusion

Phase-space methods were used to evaluate the mass-selective ion confinement properties of the rf quadrupole trap, of characteristic dimension $r_0 = 0.54$ cm, with phase-synchronization for pulsed ion injection from an external source. Singly charged ions of 10 eV energy and of mass in the neighborhood of 100 amu were considered. The injected ion beam is assumed to be well collimated with a circular cross section of 1 mm in diameter and a pulse duration of 1 μs. The quadrupole field is switched on with the rf driving voltage at a particular phase after a chosen time delay from the instant when the leading ions of the pulsed ion beam just arrived at the injection aperture. Ion injections along the gap and through an aperture on one of the electrodes were considered. A narrow mass window, sufficient for separating ions of mass numbers 99 and 101 from the ions of mass 100, is obtained by allowing a field-free drift distance between the region of ion creation and the trap injection aperture. In order to have better mass selectivity of the confined ions at the same drift distance the value of the initial rf phase should be chosen such that the corresponding time delay interval, as determined by the intersections of the unperturbed ion trajectory and the critical volume for ion confinement, is minimal at the ion mass of interest. This is contrary to choosing the initial rf phase so that the time delay interval for ion confinement is maximum to achieve high overall cross-sectional efficiency of ion confinement. By using the present scheme, i.e. the injection of a pulsed ion beam from an external source, mass-selective ion storage is possible for any operation point, within the stability region, of the rf quadrupole trap. However, different trap operation points lead to different mass selective behaviors. Operating the trap at the mass-selective tip of the stability region gives higher mass resolution but lower ion confinement efficiency.

The results presented here can be used for other traps of a different size characterized by r_0' and operated at a different angular frequency Ω', for ions of different charge e' but the same mass range after some scaling procedures. The *dc* bias U_0 and the rf driving amplitude V_0 must be changed to arrive at the same values for the stability parameters to ensure the same operation point of the quadrupole trap. Both of these voltages have to be scaled by the factor $(r_0'^2\Omega'^2/e')/(r_0^2\Omega^2/e)$. In addition, the ion energy must be modified according to $(r_0'\Omega'/r_0\Omega)^2$ to obtain the same ion injection velocity as in this paper. The situation is slightly more complicated for ions of a different mass range because the trap operation points, and therefore the phase-space ellipse parameters, are then different. For lighter mass ions the spread in the operation point due to neighboring mass numbers is much larger. This fact together with the broader velocity spread associated with ions of lower masses but the same energy and the lower mass resolution required makes it easier to selectively store ions of neighboring isotopes of the same element. The opposite is true for ions in the higher mass range because of the closer spacing of the corresponding trap operation points, the small velocity spread, and the much higher mass resolution needed.

Acknowledgements. This work was supported by the U.S. Department of Energy, the U.S. National Science Foundation, and the Center for Energy and Mineral Resources at Texas A & M University.

References

1. H.J.Kluge: In *Progress in Atomic Spectroscopy*, ed. by W.Hanle and H.Kleinpoppen, (Plenum Press, New York 1979) p. 727
2. E.-W.Otten: In *Future Directions in Studies of Nuclei far from Stability*, Proc. Int. Symp. Nashville (North-Holland, Amsterdam 1980)
3. H.L.Ravn: Phys. Rep. **54**, 201 (1979)
4. P.G.Hansen: Annu. Rev. Nucl. Sci. **29**, 69 (1979)
5. H.A.Schuessler: Physics Today **34**, 48 (Feb. 1981)
6. R.Mann, H.F.Beyer, F.Folkmann: Phys. Rev. Lett. **46**, 646 (1981)
7. F.Buchinger, W.Klempt, A.C.Mueller, E.-W.Otten, C.Ekstroem, J.Heinemeier, R.Neugart: Proc. V Int. Conf. on Hyperfine Interactions Berlin (1980)
8. J.Lindhard, M.Scharff, H.E.Schiott: Mat Fys. Medd. Dan. Vid. Solsk. **33**, 1 (1963)
9. H.G.Dehmelt: Adv. At. Mol. Phys. **3**, 53 (1967); **5**, 109 (1969)
10. H.A.Schuessler: In *Progress in Atomic Spectroscopy*, ed. by W.Hanle and H.Kleinpoppen (Plenum Press, New York 1979) p. 999
11. M.Baril, A.Septier: Rev. Phys. Appl. **9**, 505 (1974)
12. P.H.Dawson, C.Lambert: Int. J. Mass Spectrom. Ion Phys. **16**, 269 (1975)
13. G.Rettinghaus: Z. Angew. Phys. **22**, 321 (1967)
14. E.Fischer: Z. Physik **156**, 1 (1959)
15. P.H.Dawson, N.R.Whetten: J. Vac. Sci. Technol. **5**, 1 (1968)
16. C.-S.O, H.A.Schuessler: J. Appl. Phys. **52**, 1157 (1981)
17. C.-S.O, H.A.Schuessler: Int. J. Mass Spectrom. Ion Phys. **40**, 53 (1981)
18. J.F.J.Todd, D.A.Freer, R.M.Waldren: Int. J. Mass Spectrom. Ion Phys. **36**, 371 (1980)